Packaging Technology and Science

WILEY

Packaging Technology and Science
An International Journal

RESEARCH ARTICLE OPEN ACCESS

Characterization of a Food-Safe Colorimetric Indicator Based on Black Rice Anthocyanin/PET Films for Visual Analysis of Fish Spoilage

Maryam Ameri[1] | Abdellah Ajji[1] | Samuel Kessler[2]

[1]Chemical Engineering Department, Polytechnique Montréal, Montréal, Québec, Canada | [2]Active/Intelligent Packaging, ProAmpac, Cincinnati, Ohio, USA

Correspondence: Abdellah Ajji (abdellah.ajji@polymtl.ca)

Received: 10 January 2024 | **Revised:** 29 April 2024 | **Accepted:** 7 May 2024

Funding: The funding for this research project is gratefully acknowledged from the Natural Sciences and Engineering Research Council of Canada (NSERC), 3Spack Industrial Research Chair, Research Center for High Performance Polymer and Composite Systems (CREPEC), Chemical Engineering Department, Polytechnique Montréal, ProAmpac Flexible Packaging and Prima.

Keywords: anthocyanin | fish spoilage | on-package sensor | pH indicator | visual analysis

ABSTRACT

The safety of food products is of prime importance for consumers and manufacturers. Many means can be used to validate a food product's safety before it is consumed. This study is about the preparation, characterization and evaluation of a generally recognized as safe (GRAS) sensitive colorimetric sensor that detects volatile gases (TVB-N) resulting from fish spoilage, thus indicating the pH variation of packaged fish products. This is performed by coating a thin layer of ink sensors on the surface of the supporting matrix (corona-treated PET). Various visual pH indicators were prepared based on black rice anthocyanin as an FDA-approved dye. Black rice, which contains more than 80% cyanidin-3-glucoside, is the most prevalent anthocyanin component. Because of its low toxicity and high concentration, it can be utilized as a natural food colourant. pH indicators based on black rice can show distinct colours in various pH: from red (low pH) to violet (4–6) and deep purple/blue (6–7), blue (7–9) to yellowish/light brown (9–13) throughout the acid–base reaction by the analyte. The ink formulation was prepared by incorporating a binder system (PVOH-PEG) for higher surface wettability, a crosslinking agent (citric acid) for higher adhesion, an antifoaming agent (natural vanillin) and acetic acid as a pH fixing agent. Corona treatments affected substrate surface chemistry in this study. The samples with thermal treatment passed the ASTM D3330 tape test, the 8000 passages for dry sponge and the 25 passages for wet sponge through the abrasion method. Anthocyanin concentration in formulated ink based on calculation by UV–vis spectra is 0.240 mg/100 g. Sensitivity tests towards TVB-N gases were carried out at a temperature of 4°C to evaluate the performance of colorimetric films with formulated ink along with thermal treatment (temperature: 165°C, time: 5 min) using the volatile gases emitted by the fish sample inside the package.

1 | Introduction

Fish is one of the most perishable foods on the market, and there are serious health consequences to consuming it once it has spoiled. Evaluation and monitoring of the quality and safety of this high-priced and easily spoiled seafood makes the rapid and nondestructive detection of freshness a crucial duty. Currently, food industry utilizes various pH indicators to detect chemical changes caused by microbial growth or spoilage. By using pH indicators, which can change colours, and incorporating this technology into the packaging or even handheld devices, consumers can easily and quickly assess the freshness of the seafood they

purchase, ensuring their safety and preventing any potential health hazards. This approach increases food quality and decreases food waste [1–6].

Colorimetric indicators typically exploit pH-dependent structural changes of a chemical that shift its characteristic wavelength of absorbance. Specific gases are generated during the microbial spoiling of food products that can affect the colour of pH indicators during the acid–base interaction and can produce rancid aromas. Common markers for gas-targeting food sensors include carbon dioxide, oxygen volatile organic compounds (VOCs) and biogenic amines (BAs). Among these gases, the total volatile basic nitrogen (TVB-N) is the most present from spoilage of seafood products [7–11]. The presence of volatile amines, including trimethyl amine (TMA), dimethyl amine (DMA) and ammonia (NH_3), contributes to the distinct 'fishy' odour commonly associated with spoiled fish. In accordance with EU regulations, the spoilage threshold for TVB-N in fish is set at 35 mg per 100 g of flesh. Any concentration exceeding this limit is considered unsuitable for consumption [12]. Changes in concentration of TVB-N gases that are produced during spoilage of fish and meat products inside the package can be detected using pH indicator strategy. These indicators are composed of a pH sensor, a natural dye that reacts to pH changes with a noticeable colour shift and a dye carrier. Both components must be nontoxic, fulfil food safety regulations and be stable at the applied pH [13].

According to the literature, the use of synthetic dyes such as methyl orange, natural red, bromocresol green/purple and so forth [14] as pH indicators is limited due to their high toxicity and genotoxicity [15]. The most common pH indicators are based on natural substances that may be derived from fruits, vegetables, flowers or even food waste, such as anthocyanins [16].

Anthocyanins are a family of polyphenol-based flavonoids that have sensitive reactions, resulting in colour changes, to a broad range of pH (2–9) [17–19]. Also, they meet the safety standards of packaging materials and can introduce antimicrobial and antioxidant properties, which are relevant for food packaging applications [20]. Moreover, because anthocyanins are ionic, their molecular structure can be altered depending on the pH, resulting in varied colours and hues at different pH levels [13].

Colorimetric indications based on anthocyanins from red cabbage [21], purple sweet potato [22], blueberry [23], Roselle (*Hibiscus sabdariffa* L.)/curcumin [22], curcumin [24, 25], black carrot [26], shikonin [27, 28], purple tomato [29], black rice bran [30] and other dark purple and black vegetables [31] have been mentioned in studies. The findings revealed that the source of anthocyanin has a significant impact on its functional and physical properties [18, 32].

This study employed phantom proofers (doctor blade), a simple lab-scale flexography printing technology for immobilizing ink solutions that improves coating efficiency.

A suitable substrate is also required for the deposition of formulated ink. In this research, polyethylene terephthalate (PET) used as the selected substrate due to the many benefits associated with this polymer. These advantages are outlined below:

PET is a food-contact polymer with two hydroxyl (OH) groups, a dicarboxylic aromatic acid and two carboxyl (CO_2H) groups [33]. PET is good for flexible packaging due to its strength, barrier protection (resistance oxygen and other gases), flexibility, transparency and compatibility [34]. However, PET films have low surface tension in the range of 42–47 [dynes/cm] that might affect coating/printing adhesion [35]. Surface chemical, flame, plasma, corona discharge and laser ablation are popular procedures for substrate surface modification [36–40]. The material and final goal determine the optimum process.

In this study, the surface chemistry of the substrate has been modified with corona treatments. This objective is to improve surface adhesion, wettability, printability and coating quality. However, if the bonding of polar molecules does not happen properly, it risks adhesion failure [41, 42]. To address this issue, optimizing the power and speed of test operation could be beneficial in minimizing the risk of adhesion failure. On the other hand, to attain wetting, the surface energy of the formulated ink must be as low or lower than the surface energy of the substrate to be bonded. To achieve a satisfactory coating, it is important to consider that an increased level of hydrolysis and a higher molecular weight (MW) of PVOH, the primary binder in this formulation, can result in greater surface tension and reduced surface tension, respectively [43]. Thus, using appropriate binder can also change the adhesion properties. After selecting polymer films, the substrate's adhesion to inks and their interaction are crucial during printing.

PET show acceptable barrier properties towards oxygen; however, it is vulnerable against water vapour [44]. Crosslinking agents in the coated ink formulation can improve PET films' water vapour properties so they can be utilized directly with high-humidity food such as fish. Citric acid (CA) is FDA-approved poly-carboxylic acid. At low concentrations, CA, a non-toxic acid, can provide COOH groups, crosslink polysaccharides, and produce a chemical bridge between the OH groups of PVOH. To put it simply, the carboxylic groups in CA and alcoholic groups in PVOH can react to produce ester groups and water (Fischer's esterification) [45], which can be dissipated by thermal treatment or drying channels during the printing process, making coated films less susceptible to humidity. Adding a cobinder like polyethylene glycol (PEG) can help bridge PVOH chains and reduce coated films' water susceptibility [46–49].

The pH indicator that was developed in this research study is affordable, user-friendly, nondamaging and widely accessible. However, the precision of their findings is frequently imprecise due to the absence of quantitative data [50]. Additionally, there is a possibility of chemical migration from the sensor to the food. Therefore, in this study, we followed the formulation guidelines specified in the FDA-approved regulations to demonstrate the practicality of using this pH indicator on packaging for real application. The effect of thermal treatment on the response time of different types of pH indicators with different ink formulations was investigated. Finally, flexible PET films coated with natural dyes, as air-type packaging, serve as a pH-responsive sensor, exhibit precise visual variations at different pH values and show high sensitivities to TVB-N gases, which can effectively detect fish deterioration and provide valuable information to customers or sellers about the fish quality.

2 | Materials and Methods

2.1 | Materials

Starch/LLDPE (linear low-density polyethylene), starch/HDPE (high density polyethylene) and PET films are all received from ProAmpac flexible packaging company, Terrebonne, Quebec, Canada. Black rice extract 80% is from Dongguan Xiherbs Phytochem Co. Ltd, China. Polyvinyl alcohol (87%–88% hydrolysis, 145 000 MW), PEG (peg 400), CA (ACS reagent, ≥99.5%), vanillin (natural, ≥97%, FCC, FG), hydrochloric acid (HCL), acetic acid, methanol, sodium acetate ($C_2H_3NaO_2$), potassium carbonate (K_2CO_3), ammonium hydroxide solution (30%–33% NH_3 in H_2O), dimethylamine solution (40 wt.% in H_2O), trimethylamine solution (43.0%–49.0% in H2O) and potassium chloride (KCL) are from Sigma-Aldrich, Canada. Table 1 displays the components used in formulating the ink for this project.

2.2 | Senor Ink Preparation

A heterogeneous mixture composed of PVOH (5.08 g) and deionized water (39 mL) was obtained by mixing the substances inside a glass beaker. Once covered with aluminium foil to avoid contamination, the beaker was placed on the magnetic stirrer for mixing at 80°C with high speed (800 rpm) for 2 h. To overcome the foaming effect, a 10% (wt./v) solution of vanillin in 95% ethanol was added to the binder solution. After the solution cooled at room temperature while being stirred constantly, a solution mixer made of 8.69% (wt./wt. of PVOH) PEG, 22.7% (wt./wt. of PVOH) CA, 0.56 g (80%) black rice and 20-mL (wt./wt. of PVOH) DI water was added as a solvent. At the last step, between 50 and 100 μL of acetic acid was added to the final solution to fix pH of the formulated ink. The pH of solution was recorded in pH meter (Meter Toledo, Five easy plus TM, Switzerland). To have acceptable coating process, it should consider that higher degree of hydrolysis and higher MW for PVOH as main binder in this formulation, can cause larger surface tension and smaller surface tension, consecutively.

2.3 | Sensor Preparation

The coating process was performed by using TQC Automatic Film Applicator (lab-scale process of flexography printing). Different amount of final solution was coated on machine direction (MD) of corona-treated PET side MD. The speed of blade and the rod number was 75 mm/s and 60 U, respectively, which can load more ink through each passage. The prepared films dried in different temperature/time conditions (ambient temperature for 30 min and 165°C for 5 min). Print quality was analysed both visually (tape test) and numerically (colour system of RGB). The final thickness of wet films was calculated based on the amount of ink which used (4 mL) and PET surface size (21 mm × 297 mm).

2.4 | Characterization of pH Indicator

2.4.1 | Water Contact Angle (WCA) Measurements

The effect of the corona treatment on surface energy has been evaluated using contact angle measurements conducted by the sessile drop method, employing optical tensiometers from Polytechnique Montreal, as well as the dyne pen technique. The sessile drop method involves the use of a precision syringe for carefully dropping a small volume (a few μL) of probe liquid onto a flat substrate positioned on a platform. The droplet is captured in a cross-sectional view by a camera with great resolution. The determination of the static contact angle, denoted as θ, at the three-phase line of contact relies on the fitting of the drop profile, often using the Young-Laplace equation [51]. WCA for starch/LLDPE, starch/HDPE, starch/PBAT and PET films was determined using the contact angle and surface tension analyser at ambient temperature and relative humidity of %30.

2.4.2 | Tape Test

Peel testing was conducted to ensure the presence of proper adhesion bonding between the coating and its respective surface.

TABLE 1 | The ingredients utilized in the production of the ink formulation of this study, along with their corresponding FDA/GRAS status.

Material	Function	FDA status
Black rice anthocyanin (BC)	Natural dye	Anthocyanins are approved for use as food and cosmetic colourants in the EU with E number 163.
Polyvinyl alcohol (PVOH)	Binder	GRAS and FDA-approved
Polyethylene glycol (PEG)	Cobinder	May be safely used in food in accordance with some terms and conditions[a]
Citric acid (CA)	Crosslinking agent	GRAS when used in food and skin product
Vanillin	Antifoaming	In general, three types of vanillin, namely, natural, biotechnological and chemical/synthetic, are available on the market. However, only natural and nature-identical (biotechnologically produced from ferulic acid only) vanillin is considered as food-grade additives by most food-safety control authorities worldwide.
Citric acid	Fixing agent	GRAS

[a]It contains no more than 0.2% total by weight of ethylene and diethylene glycols.

In this test, a sample of the tape (Tartan 369, Polytechnique Montreal) being tested is applied to a substrate material and allowed to adhere for a specified amount of time. The tape is then peeled back at a specified angle and speed. According to the ASTM D3330, the specified value of 0.619552 lb/in. is the minimum average peel adhesion strength required for a tape to pass this test [52]. This means that if a tape's average peel adhesion strength is lower than this quantity, it fails the test. The test method used was single coated tape-peel adhesion 180 angle. The sample size is 24 mm (width), and the length is 300 mm. The dwell time was 1 min.

2.4.3 | Abrasion Test

The Linear Abrader-model 5750 were used for abresion test. The effect of drying and type of coating on the PET films investigated. The type of dry and wet sponge was 133447 from Taber Industries (New York, USA). The test was performed in the standard laboratory atmosphere of 23 ± 2°C with 50 ± 5% relative humidity. The speed is 25 (cycles/minutes), and the stroke length is 2 in.

2.4.4 | Fourier-Transform Infrared Spectroscopy (FTIR-ATR)

The FTIR spectra of the samples were recorded at room temperature using a Perkin Elmer FT-IR spectrometer 65 coupled to an ATR accessory, with a diamond crystal (Polytechnique Montreal, CA). The data were collected using Perkin Elmer spectrum. The dry starches were clamped directly onto the crystal for analysis, and the spectra were acquired in the range 4000–600 cm^{-1}, with 16 accumulations and a resolution of 16 cm^{-1}.

2.4.5 | The Spectral Characteristics of the Ink Formulation

Using a UV–Vis Spectrophotometer (Device infinite M200, Tecan, Polytechnique Montreal, CA) and the pH differential method, the total anthocyanin content of roasted black rice in the ink was found to be 0.240 mg/g. Briefly, the samples need to be diluted in the 0.025-M KCl solution adjusted to pH 1 until the $\lambda_{vis\text{-}max}$ is within the linear range of the instrument. A separate sample needs to be prepared with the same dilution factor in the 0.4 M $C_2H_3NaO_2$ solution adjusted to pH 4.5. After 15 min, the A $\lambda_{vis\text{-}max}$ and A_{700} nm are measured against a water blank [53, 54]. The following formula was used to calculate the anthocyanin pigment concentrations expressed as cyanidin-3-glucoside equivalents [13] (Equation 1):

$$\text{Monomeric anthocyanin (mg / L)} = A \times MW \times D_f \times 1000 / e \times l \quad (1)$$

where $A = \left(l_{vis-max} - A_{700\text{nm}}\right)_{pH1} - \left(l_{vis-max} - A_{700\text{nm}}\right)_{pH4.5}$, MW = molecular weight (449.2 g/mol) for cyanidin-3-glucoside (cyd-3-glu), D_f = dilution factor and e = molar extinction coefficient (28 000 L/cm.mol) for cyd-3-glu; 1000 is a factor for conversion from g to mg, and L = pathlength in cm.

2.4.6 | Colour Parameters: RGB

To evaluate the sensitivity of ammonia gas towards colorimetric platform, 3 cm × 2 cm of the film was cut, and we put it inside the container (600 mL) with one inlet in ordering inject the different volume (1, 5, 10 and 25 μL) of (30%–33%) NH_3 in H_2O at ambient temperature. The studied compound automatically volatilized and exposed to the sensor platform, which was positioned at the wall of the sealed container. Colour responses of the colorimetric film to ammonium hydroxide were captured by the scanner (Epson Canada Ltd, Perfection V550). The pictures and colorimetric information of the films were registered every 2 min (till 1 h) and after that each 1 h till 24 h as mentioned at [22] with modifications. Image analysis was performed by using MATLAB software 2019b. A desired pixel includes row, column and neighbourhood window (the window size around the pixel), were considered from pictures that we took by scanner from pH indicator. The test run for 3 different spots (pixels and considering their neighbourhood) inside each picture and the mean and standard deviation calculated. Control sample choose as reference image for RGB calculation. The colour change of pH indicators during storage period is measured by the total colour difference (ΔRGB) according to the following equation [13]:

$$\Delta\text{RGB} = \sqrt{\left(R - R_0\right)^2 + \left(G - G_0\right)^2 + \left(B - B_0\right)^2} \quad (2)$$

where R_0, B_0 and G_0 are the initial colour parameters of indicators and R, G and B were the values at the time of sampling.

2.5 | Statical Analysis

The results are reported as the average value ± standard deviation (SD).

3 | Results and Discussions

3.1 | WCA

The effect of the corona treatment on surface energy has been evaluated using contact angle measurements conducted by the sessile drop method and dyne pen. As shown in Table 2 among different trial films, PET (film thickness = 12 micron) was the most reliable film packaging material in this context because it showed a lower contact angle result compared to 25% starch/75% HDPE and 40% starch/60% LLDPE and had the lowest sensitivity towards water (compared to the films that have starch). After corona treatment of the PET films, there was a decrease in its contact angle as 104.43 ± 1.45 (±1.39%) to 65.56 ± 6.674 (±10.18%) and surface energy increased from 42 to 50 dynes/cm, respectively.

Surface coatings were applied right away after corona treatment procedure on the surface of PET films. WCA measurements were then taken before and after coating the designed ink to examine the effect of eliminating water from samples and the number of passes on adhesion properties. Corona surface treatment and addition of black rice decreased the WCA of the PET film significantly ($p < 0.05$), due to the temporary introduction of hydrophilic functional groups such as −OH and −COOH and

TABLE 2 | Analysis of variance of WCA measurements on films.

Type of films	*N*	Mean	Variance	Standard deviation	The standard error of the mean (SEM)	Margin of error at confidence level 95%
25% starch, 75% HDPE	3	113.46	1.10	1.05	0.60	113.4667 ± 1.192 (±1.05%)
40% starch, 60% LLDPE	3	106.1	3.08	1.75	1.01	106.1 ± 1.988 (±1.87%)
PET	3	104.43	1.64	1.28	0.73	104.4333 ± 1.45 (±1.39%)
PET: sealant layer						
PET corona treated	3	65.56	34.78	5.89	3.40	65.5667 ± 6.674 (±10.18%)
After coating ink formulation						
INK I-NTT-1st passage	3	51.53	12.86	3.58	2.07	51.5333 ± 4.059 (±7.88%)
INK I-NTT 2nd passage	3	56.83	0.37	0.61	0.35	56.8333 ± 0.693 (±1.22%)
INK I-165-5 1st passage	3	55.46	0.16	0.41	0.23	55.4667 ± 0.465 (±0.84%)
INK I-165-5 2nd passage	3	58.46	3.16	1.77	1.02	58.4667 ± 2.012 (±3.44%)

Note: The droplet volume is 2 μL.
Abbreviation: NTT, films without thermal treatment procedures.

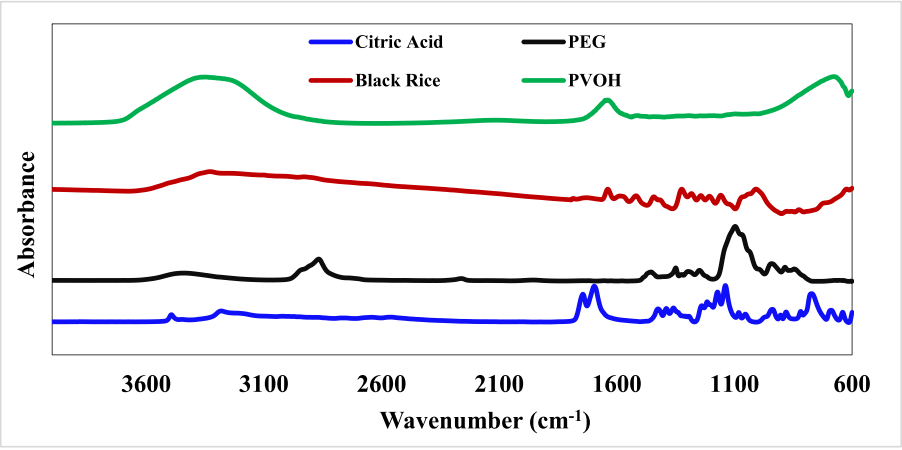

FIGURE 1 | FTIR-spectra of each component of formulated ink solution.

hydrophobic nature of black rice. According to the results, thermal treatment decreases sample water sensitivity, which can increase slightly the contact angle. This effect can be enhanced by increasing coating thickness (number of passes). Films are considered hydrophilic when the WCA is less than 65°C [55]; according to this criterion, the developed pH indicators films still can be considered hydrophilic films.

3.2 | Validation of Interaction Between Functional Groups for Better Adhesion Properties via FTIR

FTIR tests were applied to confirm the presence of hydroxyl groups, carboxylic groups and ester groups. As shown in Figure 1, the ink components' samples (PVOH, black rice, PEG and CA) and, in Figure 2, the colorimetric platform samples (Ink I-NTT and Ink I-165-5) all showed similar behaviour, with bands in the region of 3400–3200 cm^{-1}, which were assigned to the stretching vibration of the O-H group.

3.2.1 | Formulated Ink

The bands at 1638 (C-O stretching) and 1572/1517 are related to protein content of roasted black rice. The bands at 1441–1323 cm^{-1} were assigned to C-H bending vibrations, while the band at 1242 cm^{-1} was ascribed to the O-H bending vibrations [43]. The bands at 1157 and 1008 cm^{-1} corresponded to the ring vibrations juxtaposed with the stretching vibrations of the lateral groups (C-OH) and to C-O-C glycoside vibrations. The

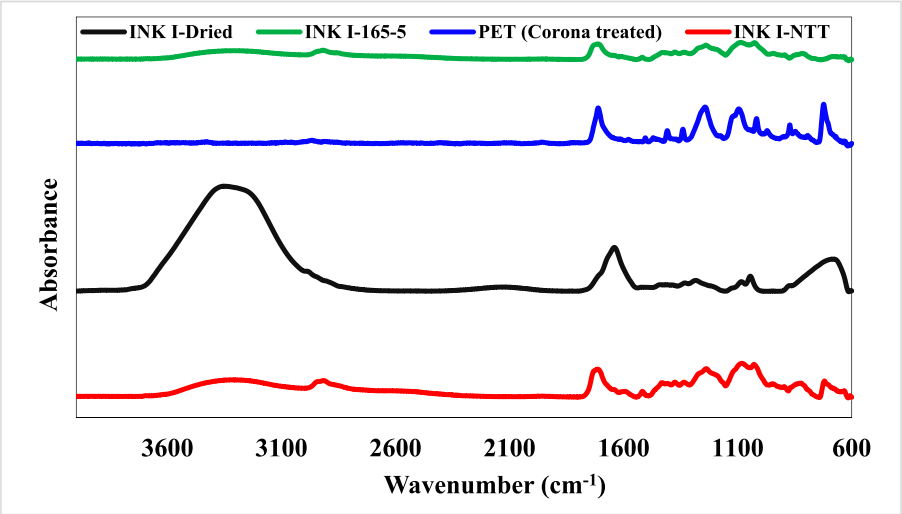

FIGURE 2 | FTIR spectra of dried solution ink (INK I-Dried), fabricated colorimetric films with thermal treatment (INK I-165-60) and without thermal treatment (INK-I-NTT) and sealant layer (PET corona treated).

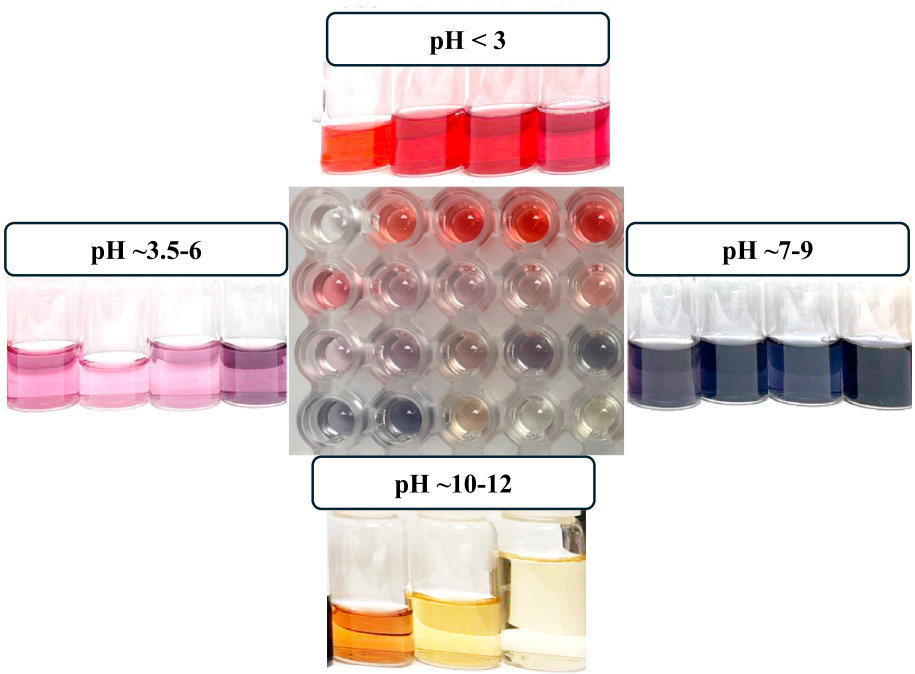

FIGURE 3 | The colour alternation of black rice anthocyanin at various pH.

observed peaks have confirmation with [56]. By adding black rice in ink formulation, the peak intensity for OH groups increased and shifted to higher wavelength. This shift could indicate a change in the chemical environment of the OH group. Explanation for this shift could be changes in polarity or hydrogen bonding in the molecule, changes in the temperature of the system being analysed or changes in the solvent or pH.

3.2.2 | Colorimetric Platform

There is a new peak at 2919 cm^{-1} in coated PET films with INK I formulation, which may be due to the presence of PEG, causing an additional bridge between PVOH groups. The intensity of hydroxyl bands decreases significantly after heat treatment of samples, indicating transitory water loss and a lower number of accessible water molecules from hydrogen bonding because of dehydration. This suggests that the crosslinking was caused by the solvent and alcohol that leaked from the samples, as well as the presence of CA as a crosslinking agent. The absorption of 1713 cm^{-1} was assigned to a C = O stretching vibration and could be attributed to the carbonyl groups in coated film. Also, the $\Delta A = 0.02$ for peak 1713 cm^{-1} (C=O) stretching for the INK I-165-5 intensified. The band at 1230 cm^{-1}, which is connected to the ester C-O stretching (Fisher's esterification), also supports the esterification [57]. This peak can demonstrate that crosslinking between CA and PVOH occurred.

3.3 | Validation of Adhesion: Tape Test and Abrasion Test

According to the tape test and abrasion results from several types of PET films coated with these different ink formulations based on black rice and PVOH, films without thermal treatment or with insufficient thermal treatment (90°C for 60 min, 50°C for 24 h and 145°C for 15 min) would remove more area, which we did not present results here. The classification of adhesion results was based on the D3359-17 standard [52], in which at least 5%–15% of the coating of samples without thermal treatment was removed when it comes to contact with water (as fish packages have high humidity). Final samples with proper thermal treatment (165°C for 5 min) passed the tape test [52]. Also, these samples passed the abrasion test with 4000 cycles for dry sponge and 25 cycles for wet sponge. Thus, applying the correct thermal treatment to the samples can enhance their adhesion qualities, hence enabling the colorimetric platform to function effectively.

3.4 | UV–vis Spectra of the Ink Solution at Different pHs and Its Stability

A spectrophotometric titration using a deprotonation–protonation process was performed and monitored at $\lambda = 520$ nm (which sample showed maximum absorbance). The Ink I formulation was diluted using DI water until it reached an absorbance of 1.0271 at 510 nm. This was placed in 20-mL disposable scintillation vials at 23°C, protected from light and kept under constant vortex. Aliquots of ammonium hydroxide 0.1 M and HCL 1 N were added to the diluted ink, and every change of 0.5 in pH, the absorbance was recorded at 520 nm until a pH 10 was reached. (Device infinite M200, Tecan).

The influence of pH to the anthocyanin colour stability was investigated by the absorbance of UV light with a wavelength of 400–700 nm, using UV–VIS spectrophotometer. Roasted black rice showed obvious colour changes in different buffers [56]. Black rice is rich in various anthocyanins, such as cyanidin-3-glucoside (acidic conditions), delphinidin-3-glucoside (neutral pH) and petunidin-3-glucoside (alkine conditions) [58]. The chemical structure of these molecules can change based on the pH levels, influencing the colour changes in black rice. Simply explained, the anthocyanin underwent a chemical process that produced a new molecular species (from flavylium cation to hemiketal or quinoidal) with altered absorption characteristics [59, 60]. To detect flavonoids in the prepared ink solution, a few droplets of HCl added to 10 mL of anthocyanin solution, which causes a red solution [59]. In Figure 3, the colour alternation of black rice anthocyanin at various pH is depicted.

The colour change at pH 2–12 was indicated by the change of the distinctive absorbance at a certain maximum wavelength for each sample at each pH condition. The absorption spectrum of the natural pigment anthocyanin covers the entire visible region, and the peak absorbance was observed at 510 nm. The pH for $D_f = 0.1$ is equal to 2.95, and for $D_f = 0.01$, it is equal to 3.35.

In Figure 4, UV–vis spectra of solution ink at different pHs were depicted. The change in pH (from 2 to 3.5) and molecular structure of anthocyanin inside the ink formulation caused a drop in absorbance peak intensity (at 510 nm) in the UV–visible (UV–vis) spectrum. When the pH increased to 4–6, a bathochromic shift occurred from 510 (pH 4) to 560 nm (pH 6). This shifting exhibited a purple colour due to the change of anthocyanin structure. At pH 7, the colour changed to blue because of the anionic and natural quinoidal bases. At the wavelength of 580, the colour intensity increased at sample of pH 7–10 (bluish green), while decreased from 580 to 520 at the sample with pH 10–11 and, finally, from pH 11 to 12, the intensity slightly increased suggested colour change from light brown to dark yellow [13].

3.5 | Anthocyanin Contents

In this study, anthocyanin concentrations were measured using the Giusti and Wrolstad-proposed pH differential method, which is based on the structural transformations of the anthocyanin chromophore as a function of pH. This method uses pH-dependent structural changes of the anthocyanin chromophore. At pH 4.5, the colourless hemiketal form predominates, while at pH = 1, the red flavylium form prevails. Instead of quantifying at 520 nm, the approach uses absorbance at the $l_{vis\text{-}max}$ for

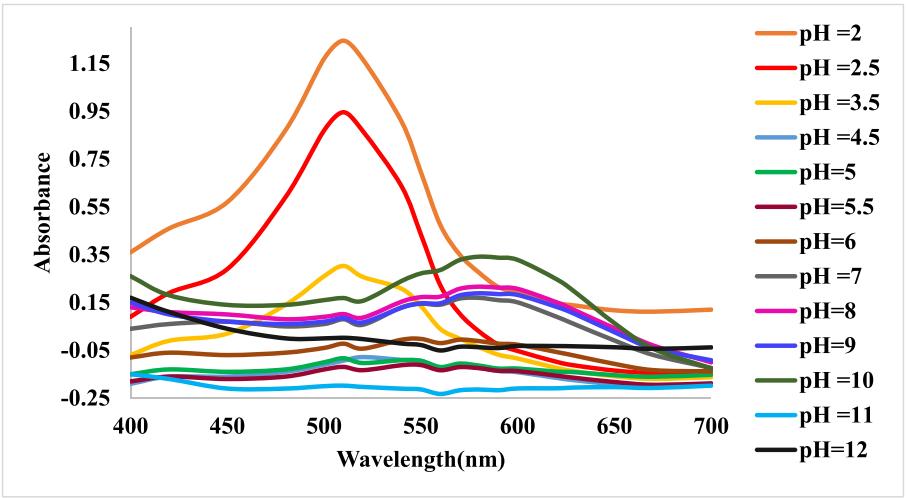

FIGURE 4 | UV–vis spectra of solution ink at different pH.

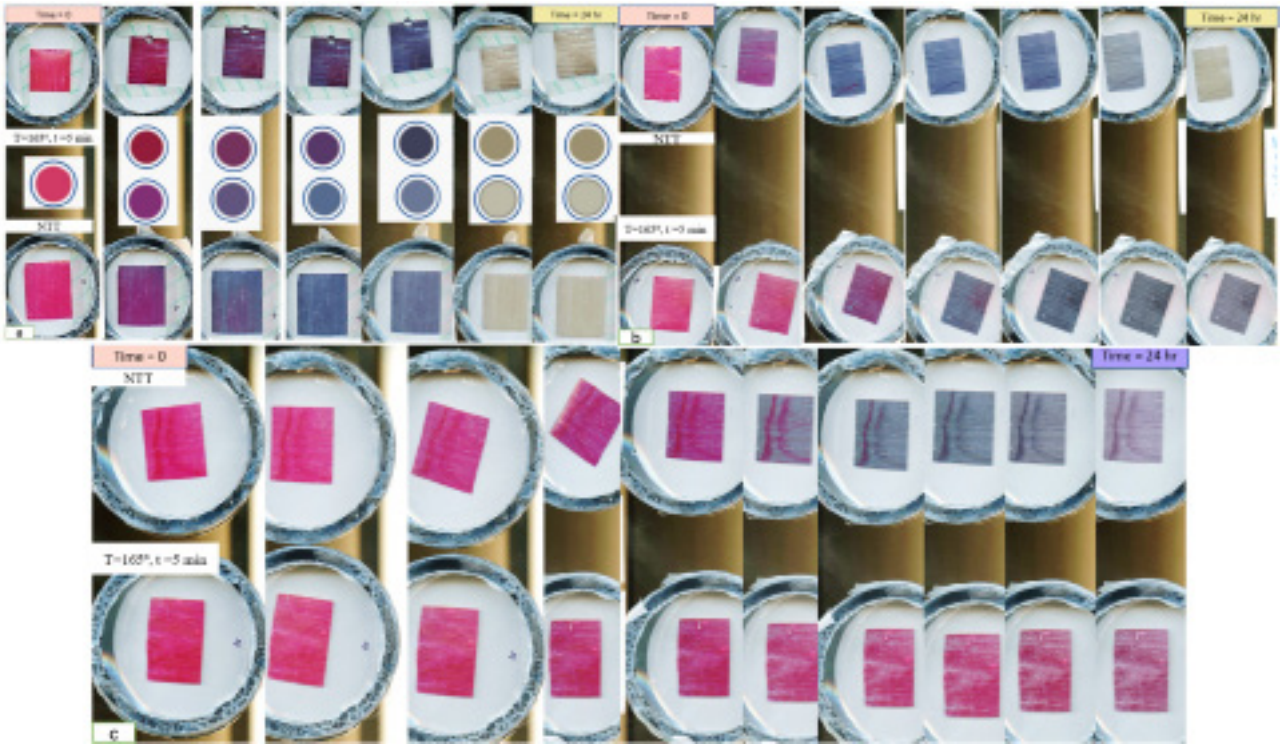

FIGURE 5 | Sensitivity test for examining the response of pH indicator towards NH_3 gases, a = 25 μL, b = 10 μL and c = 5 μL of (30%–33%) ammonium hydroxide.

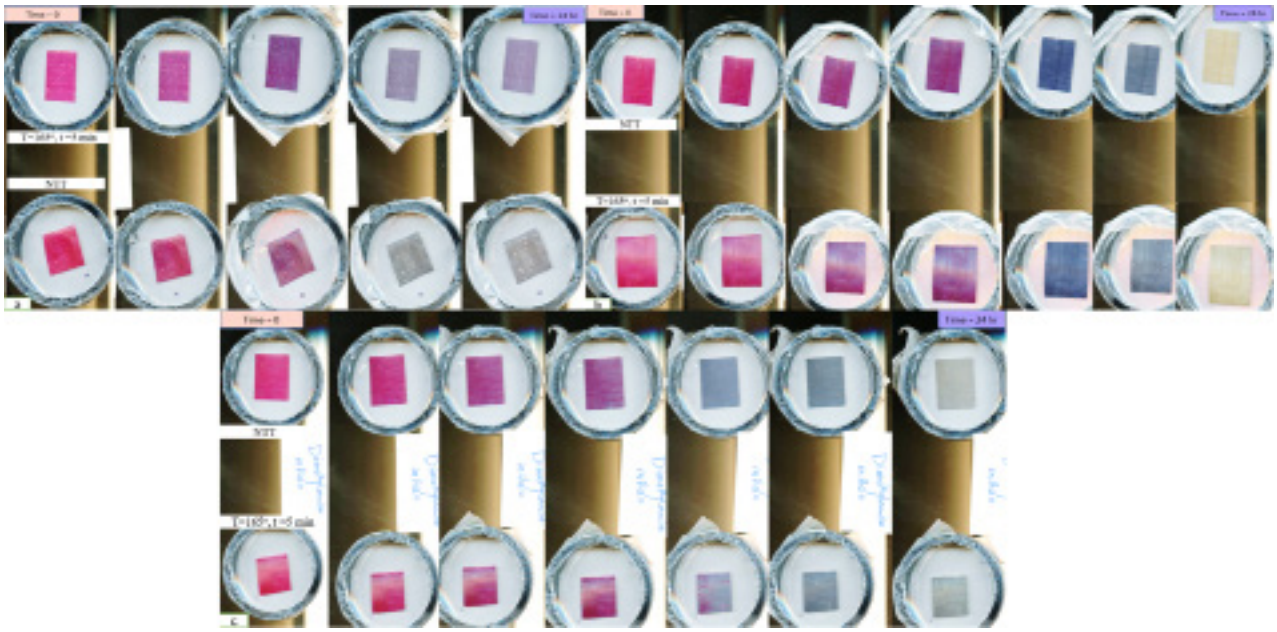

FIGURE 6 | Sensitivity test for examining the response of pH indicator towards DMA, a = 25 μL, b = 10 μL and c = 5 μL of dimethylamine solution.

precision. To avoid haze-induced light scattering, the absorbance at 700 nm was added. The approach also requires the MW and molar absorption coefficient (ε) of malvidin-3-glucoside, the sample's main anthocyanin, to calculate its total amount [54].

Worth to mention that black rice anthocyanin MW varies by component. Cyanidin-3-glucoside is one of the most prevalent anthocyanins in black rice, which has MW = 449.2 g/mol as mentioned in Equation 1. Other black rice anthocyanins have comparable MWs. According to the results, the anthocyanin content of Ink I is 0.240 mg/100 g using the above approach. The overall quantity of black rice in this formulation is approximately 0.82 mg/100 g. We should note that the result appears plausible due to pigment and dye sedimentation.

3.6 | Colour Response to Volatile Amines (Ammonia, Dimethylamine and Trimethylamine)

Colorimetric films react with the production of nitrogen-based compounds (such as NH_3, DMA and TMA) that can be utilized to check the freshness of high-protein foods like meat and fish. The change in colour of the colorimetric platform was recorded by a scanner that is linked to a computer for further analysis. The images were taken before and after exposure of ammonium hydroxide, dimethylamine solution and trimethylamine solution to the colorimetric platform for a duration of 24 h. The colour change exhibited a rapid rate, with most changes occurring within the first 15 min. Subsequently, a slower rate of change persisted for an extended duration, as seen in Figures 5–7. Additionally, it is notable that the quickest colour shift was observed in less than 1 min. The results indicate that the naked eye is unable to detect the sensitivity to 1 μL of the stock solution. However, specific details on this observation are not provided in this context. The films undergo a transition in colour, progressing from a red hue to a deep purple/blue shade and to a light brown/dark yellow tone. Dissociation of the H+ ion from a pH indicator causes its colour shift. Note that pH indicators are weak acids and natural colours. The solution changes colour when the weak acid indicator dissociates. The observed alterations in colour may be attributed to the formation of an alkaline environment around the natural dye, facilitated by the presence of NH_3 gas, which generates OH− ions upon contact with water [22]. Furthermore, it was noted that there were no discernible changes in colour detected in the coated films containing a low concentration of black rice when exposed to various kinds of ammonia gases. This may be attributed to the absence of anthocyanins in the films, as supported by previous research [56].

The assessment of the selectivity of the developed pH indicator is associated with the measurement of the ΔRGB in the presence of several VOCs at a defined concentration. Figures 5–7 demonstrate

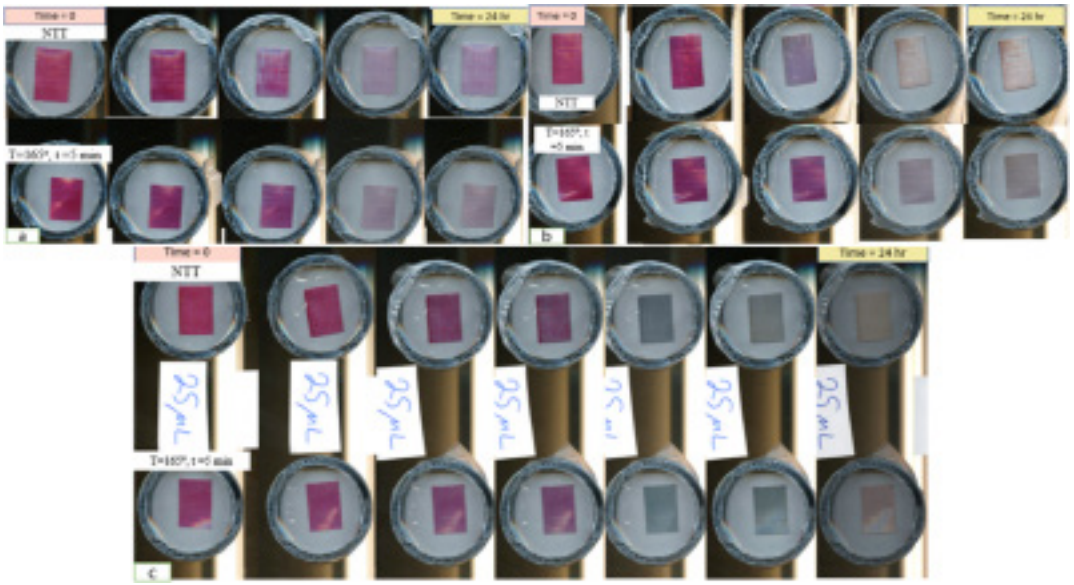

FIGURE 7 | Sensitivity test for examining the response of pH indicator towards TMA, a = 25 μL, b = 10 μL and c = 5 μL of trimethylamine solution.

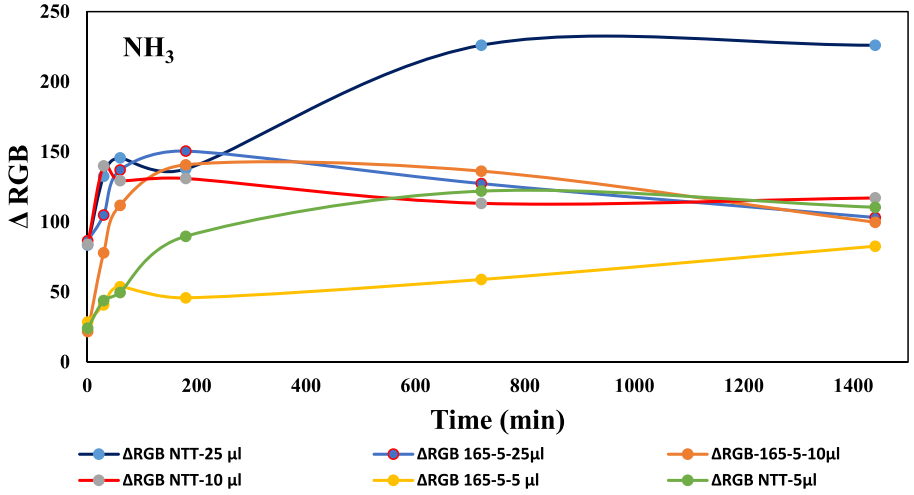

FIGURE 8 | ΔRGB results for fabricated colorimetric films with and without thermal treatment over time by exposure to the (30%–33%) ammonium hydroxide.

a notable alteration in colour upon exposure of the sensor to NH_3, DMA and TMA. In contrast, the sensor's colour exhibited no alteration upon exposure to various organic substances, including acetone, ethanol, methanol, formaldehyde and dimethylformamide.

To better understand the colour-changing behaviour of film indicators, ΔRGB for NH_3 towards time is depicted, as seen in Figure 8. In contrast to dried samples, produced indicators that have not undergone thermal treatment may exhibit a prompt colour alteration as time progresses. Compared with the fresh samples, the ΔRGB values of the dried samples were gently lowered. This phenomenon could be attributed to partially destruction of anthocyanins and its active component at elevated temperature [61]. Table 3 displays the statistical data, including the mean value of ΔRGB for three distinct pixels for each pH indicator during the time.

TABLE 3 | The mean value of ΔRGB of NH_3 for three distinct pixels for each pH indicator during the time.

Type of pH indicator and used volume	Time	ΔRGB	SD
Ink I-165-5 25 μL	1	86.51	20.33
	30	104.95	13.98
	60	137.02	9.60
	180	150.48	5.10
	720	127.33	35.71
	1440	103.12	27.80
Ink I-NTT 25 μL	1	83.45	8.16
	30	132.60	8.66
	60	145.59	4.78
	180	137.66	6.54
	720	226.02	3.63
	1440	226.02	3.63
Ink I-165-5 10 μL	1	21.722	11.30
	30	77.863	5.13
	60	111.86	4.675
	180	140.73	15.67
	720	136.23	17.07
	1440	99.73	5.41
Ink I-NTT 10 μL	1	83.92	16.62
	30	140.04	2.86
	60	129.44	8.40
	180	130.93	1.17
	720	113.23	11.42
	1440	117.07	9.69
Ink I-165-5 5 μL	1	28.50	12.06
	30	40.84	14.74
	60	53.71	15.47
	180	45.82	26.56
	720	58.89	33.93
	1440	82.65	17.05
Ink I-NTT 5 μL	1	24.09	11.88
	30	43.89	20.12
	60	49.66	9.01
	180	89.72	33.14
	720	121.92	5.34
	1440	110.39	21.17

In this study, the anthocyanin content in the thermally heated samples at 165°C was very low, but it did not disappear totally and could change colour towards NH_3 gases. Thus, the pH indicator for fish packing must adjust for lag time correction. This is particularly crucial as the samples come into direct contact with food products, ensuring that the pH sensors will stay intact due to the elevated humidity levels within the packaging.

4 | Conclusions

Colorimetric films were successfully developed by coating formulated ink, including black rice anthocyanin, on the surface of a corona-treated PET substrate. By using natural dye solutions within the pH range of 2–12, it is possible to visually see a colour change when exposed to amine base gases. These gases are generated because of microbial activity during the spoilage of meat and fish products. The FTIR spectra results indicate that the inclusion of PEG as a cobinder can lead to the formation of an additional link between the PVOH groups, validating the interaction between functional groups and enhancing the adhesion properties. The findings from the tape and abrasion tests indicate that the use of thermal treatment for colorimetric films may enhance the adhesive bonding between formulated ink and the substrate by eliminating water. Moreover, heat drying colorimetric indicators at elevated temperatures can cause anthocyanin degradation, which could result in poorer colour change. Therefore, optimization of the heating process (time and temperature) and choosing the pH level for ink formulation are two crucial parameters for developing pH indicators. Finally, the developed colorimetric film benefits from using inexpensive, readily available, and environmentally friendly dyes and an easy printing process for food packaging applications. Therefore, this approach will effectively address a significant drawback associated with on-package sensors, namely, the potential for chemical migration onto food. Additionally, the developed pH indicator demonstrated robust stability under the laboratory lamp light and room temperature, exhibiting minimal alteration throughout the duration of exposure. Also, insignificant degradation throughout high temperature for short periods of time.

Acknowledgements

The funding for this research project is gratefully acknowledged from the Natural Sciences and Engineering Research Council of Canada (NSERC), 3Spack Industrial Research Chair, Research Center for High Performance Polymer and Composite Systems (CREPEC), Chemical Engineering Department, Polytechnique Montréal, ProAmpac Flexible Packaging and Prima. We express our gratitude to Dr. Bentolhoda Heli for her academic and spiritual guidance.

Data Availability Statement

The data that support the findings will be available under the request.

References

1. W. Huang, X. Wang, J. Xia, et al., "Flexible Sensing Enabled Agri-Food Cold Chain Quality Control: A Review of Mechanism Analysis, Emerging Applications, and System Integration," *Trends in Food Science and Technology* 133 (2023): 189–204.

2. W. Sun, H. Li, H. Wang, S. Xiao, J. Wang, and L. Feng, "Sensitivity Enhancement of pH Indicator and Its Application in the Evaluation of Fish Freshness," *Talanta* 143 (2015): 127–131.

3. E. Balbinot-Alfaro, D. V. Craveiro, K. O. Lima, H. L. G. Costa, D. R. Lopes, and C. Prentice, "Intelligent Packaging With pH Indicator Potential," *Food Engineering Reviews* 11 (2019): 235–244.

4. E. Poyatos-Racionero, J. V. Ros-Lis, J.-L. Vivancos, and R. Martinez-Manez, "Recent Advances on Intelligent Packaging as Tools to Reduce Food Waste," *Journal of Cleaner Production* 172 (2018): 3398–3409.

5. J. K. Heising, G. Claassen, and M. Dekker, "Options for Reducing Food Waste by Quality-Controlled Logistics Using Intelligent Packaging Along the Supply Chain," *Food Additives & Contaminants: Part A* 34, no. 10 (2017): 1672–1680.

6. K. Pounds, S. Jairam, H. Bao, et al., "Glycerol-Based Dendrimer Nanocomposite Film as a Tunable pH-Sensor for Food Packaging," *ACS Applied Materials & Interfaces* 13, no. 19 (2021): 23268–23281.

7. J. Liu, H. Wang, M. Guo, et al., "Extract From *Lycium ruthenicum* Murr. Incorporating κ-Carrageenan Colorimetric Film With a Wide pH–Sensing Range for Food Freshness Monitoring," *Food Hydrocolloids* 94 (2019): 1–10.

8. Y. Liu, Y. Qin, R. Bai, X. Zhang, L. Yuan, and J. Liu, "Preparation of pH-Sensitive and Antioxidant Packaging Films Based on κ-Carrageenan and Mulberry Polyphenolic Extract," *International Journal of Biological Macromolecules* 134 (2019): 993–1001.

9. W. Lan, S. Wang, Z. Zhang, X. Liang, X. Liu, and J. Zhang, "Development of Red Apple Pomace Extract/Chitosan-Based Films Reinforced by TiO_2 Nanoparticles as a Multifunctional Packaging Material," *International Journal of Biological Macromolecules* 168 (2021): 105–115.

10. K. Zhang, T.-S. Huang, H. Yan, X. Hu, and T. Ren, "Novel pH-Sensitive Films Based on Starch/Polyvinyl Alcohol and Food Anthocyanins as a Visual Indicator of Shrimp Deterioration," *International Journal of Biological Macromolecules* 145 (2020): 768–776.

11. S. Kang, H. Wang, L. Xia, et al., "Colorimetric Film Based on Polyvinyl Alcohol/Okra Mucilage Polysaccharide Incorporated With Rose Anthocyanins for Shrimp Freshness Monitoring," *Carbohydrate Polymers* 229 (2020): 115402.

12. J. Kerry and P. Butler, *Smart Packaging Technologies for Fast Moving Consumer Goods* (John Wiley & Sons, 2008).

13. D. N. Dikmetas, E. Uysal, F. Karbancioglu-Guler, and S. Gurmen, "The Production of pH Indicator Ca and Cu Alginate ((1, 4)-β-d-Mannuronic Acid and α-L-Guluronic Acid) Cryogels Containing Anthocyanin Obtained via Red Cabbage Extraction for Monitoring Chicken Fillet Freshness," *International Journal of Biological Macromolecules* 231 (2023): 123304.

14. Y. S. Musso, P. R. Salgado, and A. N. Mauri, "Gelatin Based Films Capable of Modifying Its Color Against Environmental pH Changes," *Food Hydrocolloids* 61 (2016): 523–530.

15. A. Castañeda-Ovando, M. d. L. Pacheco-Hernández, M. E. Páez-Hernández, J. A. Rodríguez, and C. A. Galán-Vidal, "Chemical Studies of Anthocyanins: A Review," *Food Chemistry* 113, no. 4 (2009): 859–871.

16. P. Shao, L. Liu, J. Yu, et al., "An Overview of Intelligent Freshness Indicator Packaging for Food Quality and Safety Monitoring," *Trends in Food Science and Technology* 118 (2021): 285–296, https://doi.org/10.1016/j.tifs.2021.10.012.

17. T. C. Wallace and M. M. Giusti, "Anthocyanins—Nature's Bold, Beautiful, and Health-Promoting Colors," *Food* 8 (2019): 550.

18. H. E. Khoo, A. Azlan, S. T. Tang, and S. M. Lim, "Anthocyanidins and Anthocyanins: Colored Pigments as Food, Pharmaceutical Ingredients, and the Potential Health Benefits," *Food & Nutrition Research* 61, no. 1 (2017): 1361779.

19. G. T. Sigurdson, P. Tang, and M. M. Giusti, "Natural Colorants: Food Colorants From Natural Sources," *Annual Review of Food Science and Technology* 8 (2017): 261–280.

20. N. Oladzadabbasabadi, A. M. Nafchi, M. Ghasemlou, F. Ariffin, Z. Singh, and A. Al-Hassan, "Natural Anthocyanins: Sources, Extraction, Characterization, and Suitability for Smart Packaging," *Food Packaging and Shelf Life* 33 (2022): 100872.

21. T. Liang, G. Sun, L. Cao, J. Li, and L. Wang, "A pH and NH3 Sensing Intelligent Film Based on *Artemisia sphaerocephala* Krasch. Gum and Red Cabbage Anthocyanins Anchored by Carboxymethyl Cellulose Sodium Added as a Host Complex," *Food Hydrocolloids* 87 (2019): 858–868.

22. F. S. Mohseni-Shahri and F. Moeinpour, "Development of a pH-Sensing Indicator for Shrimp Freshness Monitoring: Curcumin and Anthocyanin-Loaded Gelatin Films," *Food Science & Nutrition* 11, no. 7 (2023): 3898–3910, https://doi.org/10.1002/fsn3.3375.

23. M. Alizadeh-Sani, M. Tavassoli, E. Mohammadian, et al., "pH-Responsive Color Indicator Films Based on Methylcellulose/Chitosan Nanofiber and Barberry Anthocyanins for Real-Time Monitoring of Meat Freshness," *International Journal of Biological Macromolecules* 166 (2021): 741–750.

24. S. Roy and J.-W. Rhim, "Preparation of Carbohydrate-Based Functional Composite Films Incorporated With Curcumin," *Food Hydrocolloids* 98 (2020): 105302.

25. P. Ezati and J.-W. Rhim, "pH-Responsive Pectin-Based Multifunctional Films Incorporated With Curcumin and Sulfur Nanoparticles," *Carbohydrate Polymers* 230 (2020): 115638.

26. M. Moradi, H. Tajik, H. Almasi, M. Forough, and P. Ezati, "A Novel pH-Sensing Indicator Based on Bacterial Cellulose Nanofibers and Black Carrot Anthocyanins for Monitoring Fish Freshness," *Carbohydrate Polymers* 222 (2019): 115030.

27. P. Ezati, Y.-J. Bang, and J.-W. Rhim, "Preparation of a Shikonin-Based pH-Sensitive Color Indicator for Monitoring the Freshness of Fish and Pork," *Food Chemistry* 337 (2021): 127995.

28. H. Dong, Z. Ling, X. Zhang, X. Zhang, S. Ramaswamy, and F. Xu, "Smart Colorimetric Sensing Films With High Mechanical Strength and Hydrophobic Properties for Visual Monitoring of Shrimp and Pork Freshness," *Sensors and Actuators B: Chemical* 309 (2020): 127752.

29. Y. Li, K. Wu, B. Wang, and X. Li, "Colorimetric Indicator Based on Purple Tomato Anthocyanins and Chitosan for Application in Intelligent Packaging," *International Journal of Biological Macromolecules* 174 (2021): 370–376.

30. C. Wu, J. Sun, P. Zheng, et al., "Preparation of an Intelligent Film Based on Chitosan/Oxidized Chitin Nanocrystals Incorporating Black Rice Bran Anthocyanins for Seafood Spoilage Monitoring," *Carbohydrate Polymers* 222 (2019): 115006.

31. H. Li, Z. Deng, H. Zhu, et al., "Highly Pigmented Vegetables: Anthocyanin Compositions and Their Role in Antioxidant Activities," *Foodservice Research International* 46, no. 1 (2012): 250–259.

32. J. Shipp and E.-S. M. Abdel-Aal, "Food Applications and Physiological Effects of Anthocyanins as Functional Food Ingredients," *The Open Food Science Journal.* 4, no. 1 (2010): 7–22.

33. E. Tsochatzis, J. A. Lopes, and M. Corredig, "Chemical Testing of Mechanically Recycled Polyethylene Terephthalate for Food Packaging in the European Union," *Resources, Conservation and Recycling* 179 (2022): 106096.

34. T. Fernández-Menéndez, D. García-López, A. Argüelles, A. Fernández, and J. Viña, "Industrially Produced PET Nanocomposites With Enhaced Properties for Food Packaging Applications," *Polymer Testing* 90 (2020): 106729.

35. V. C. Louzi and J. S. de Carvalho Campos, "Corona Treatment Applied to Synthetic Polymeric Monofilaments (PP, PET, and PA-6)," *Surfaces and Interfaces* 14 (2019): 98–107.

36. M. Lindner, N. Rodler, M. Jesdinszki, M. Schmid, and S. Sängerlaub, "Surface Energy of Corona Treated PP, PE and PET Films, Its Alteration as Function of Storage Time and the Effect of Various Corona Dosages on Their Bond Strength After Lamination," *Journal of Applied Polymer Science* 135, no. 11 (2018): 45842, https://doi.org/10.1002/app.45842.

37. L. Penn and H. Wang, "Chemical Modification of Polymer Surfaces: A Review," *Polymers for Advanced Technologies* 5, no. 12 (1994): 809–817.

38. S. Siau, A. Vervaet, A. Van Calster, I. Swennen, and E. Schacht, "Influence of Wet Chemical Treatments on the Evolution of Epoxy Polymer Layer Surface Roughness for Use as a Build-Up Layer," *Applied Surface Science* 237, no. 1–4 (2004): 457–462.

39. E. Liston, L. Martinu, and M. Wertheimer, "Plasma Surface Modification of Polymers for Improved Adhesion: A Critical Review," *Journal of Adhesion Science and Technology* 7, no. 10 (1993): 1091–1127.

40. C. J. Wohl, M. A. Belcher, S. Ghose, and J. W. Connell, "Modification of the Surface Properties of Polyimide Films Using Polyhedral Oligomeric Silsesquioxane Deposition and Oxygen Plasma Exposure," *Applied Surface Science* 255, no. 18 (2009): 8135–8144.

41. C. Sun, D. Zhang, and L. C. Wadsworth, "Corona Treatment of Polyolefin Films—A Review," *Advances in Polymer Technology: Journal of the Polymer Processing Institute.* 18, no. 2 (1999): 171–180.

42. P. Fabbri and M. Messori, "Surface Modification of Polymers: Chemical, Physical, and Biological Routes," in *Modification of Polymer Properties*, (William Andrew, 2017), 109–130.

43. W.-B. Chu, J.-W. Yang, T.-J. Liu, C. Tiu, and J. Guo, "The Effects of pH, Molecular Weight and Degree of Hydrolysis of Poly (Vinyl Alcohol) on Slot Die Coating of PVA Suspensions of TiO_2 and SiO_2," *Colloids and Surfaces A: Physicochemical and Engineering Aspects* 302, no. 1–3 (2007): 1–10.

44. J. Sarfraz, T. Gulin-Sarfraz, J. Nilsen-Nygaard, and M. K. Pettersen, "Nanocomposites for Food Packaging Applications: An Overview," *Nanomaterials* 11, no. 1 (2021): 10, https://doi.org/10.3390/nano11010010.

45. E. Y. Malikov, M. B. Muradov, O. H. Akperov, et al., "Synthesis and Characterization of Polyvinyl Alcohol Based Multiwalled Carbon Nanotube Nanocomposites," *Physica E: Low-Dimensional Systems and Nanostructures.* 61 (2014): 129–134.

46. D. Urban, B. Schuler, and J. Schmidt-Thümmes, "Large Volume Applications of Latex Polymers," in *Chemistry and Technology of Emulsion Polymerisation*, (Wiley, 2013), 253–282.

47. W. J. Auhorn, "Chemical Additives," in *Handbook of Paper and Board*, (Wiley, 2006), 62–149.

48. S. Lorca, F. Santos, and A. J. Fernández Romero, "A Review of the Use of GPEs in Zinc-Based Batteries. A Step Closer to Wearable Electronic Gadgets and Smart Textiles," *Polymers* 12, no. 12 (2020): 2812, https://doi.org/10.3390/polym12122812.

49. J. Laine, "Effect of Synthetic Modifiers on the Rheology of Coating Colours" (2015).

50. B. Kuswandi, M. Moradi, and P. Ezati, "Food Sensors: Off-Package and On-Package Approaches," *Packaging Technology and Science* 35, no. 12 (2022): 847–862.

51. Y. Yuan and T. R. Lee, "Contact Angle and Wetting Properties," in *Surface Science Techniques*, (Verlag, Berlin, Heidelberg: Springer, 2013), 3–34.

52. S. Tape, "Standard Test Methods for Rating Adhesion by Tape Test1".

53. J. Lee, R. W. Durst, R. E. Wrolstad, et al., "Determination of Total Monomeric Anthocyanin Pigment Content of Fruit Juices, Beverages, Natural Colorants, and Wines by the pH Differential Method: Collaborative Study," *Journal of AOAC INTERNATIONAL* 88, no. 5 (2005): 1269–1278, https://doi.org/10.1093/jaoac/88.5.1269.

54. M. M. Giusti and R. E. Wrolstad, "Acylated Anthocyanins From Edible Sources and Their Applications in Food Systems," *Biochemical Engineering Journal* 14, no. 3 (2003): 217–225, https://doi.org/10.1016/S1369-703X(02)00221-8.

55. E. A. Vogler, "Structure and Reactivity of Water at Biomaterial Surfaces," *Advances in Colloid and Interface Science* 74, no. 1–3 (1998): 69–117, https://doi.org/10.1016/S0001-8686(97)00040-7.

56. H. Yong, J. Liu, Y. Qin, R. Bai, X. Zhang, and J. Liu, "Antioxidant and pH-Sensitive Films Developed by Incorporating Purple and Black Rice Extracts Into Chitosan Matrix," *International Journal of Biological Macromolecules* 137 (2019): 307–316.

57. A. Musetti, K. Paderni, P. Fabbri, A. Pulvirenti, M. Al-Moghazy, and P. Fava, "Poly (Vinyl Alcohol)-Based Film Potentially Suitable for Antimicrobial Packaging Applications," *Journal of Food Science* 79, no. 4 (2014): E577–E582.

58. R. Cortez, D. A. Luna-Vital, D. Margulis, and E. Gonzalez de Mejia, "Natural Pigments: Stabilization Methods of Anthocyanins for Food Applications," *Comprehensive Reviews in Food Science and Food Safety* 16, no. 1 (2017): 180–198.

59. M. E. El-Naggar, M. H. El-Newehy, A. Aldalbahi, W. M. Salem, and T. A. Khattab, "Immobilization of Anthocyanin Extract From Red-Cabbage Into Electrospun Polyvinyl Alcohol Nanofibers for Colorimetric Selective Detection of Ferric Ions," *Journal of Environmental Chemical Engineering* 9, no. 2 (2021): 105072.

60. J.-M. Kong, L.-S. Chia, N.-K. Goh, T.-F. Chia, and R. Brouillard, "Analysis and Biological Activities of Anthocyanins," *Phytochemistry* 64, no. 5 (2003): 923–933.

61. J. Wang, G. Wu, Z. Wang, et al., "The Influence of Processing Conditions on Kinetics, Anthocyanin Profile and Antioxidant Activity of Purple Sweet Potato Subjected to Hot Air Drying," *Journal of Food Process Engineering* 43, no. 9 (2020): e13472.

Supporting Information

Additional supporting information can be found online in the Supporting Information section.